

## Absorption Spectra, $pK_a$ , and Reduction Potential of Phenoxyl Radical from 4,4'-Biphenol in Aqueous Medium

Tomi Nath Das\*

Radiation Chemistry & Chemical Dynamics Division, B.A.R.C., Trombay, Mumbai 400 085, India

Received: December 22, 2000; In Final Form: March 28, 2001

The optical absorption spectra,  $pK_a$ , and one-electron reduction potential ( $E^1$ ) of the phenoxyl radical of 4,4'-biphenol ( $\text{HOArArOH}$ ;  $\text{Ar}=\text{C}_6\text{H}_4$ ) in aqueous solution are measured by the pulse radiolysis technique. At pH 4.8 the absorption spectrum of the  $\text{HOArArO}^\cdot$  radical shows two peaks at 385 nm ( $\epsilon = 2223 \text{ m}^2 \text{ mol}^{-1}$ ) and 620 nm ( $\epsilon = 867 \text{ m}^2 \text{ mol}^{-1}$ ). At pH 12.0, the respective peaks due to the  $^-\text{OArArO}^\cdot$  radical appear at 445 nm ( $\epsilon = 2850 \text{ m}^2 \text{ mol}^{-1}$ ) and 730 nm ( $\epsilon = 1680 \text{ m}^2 \text{ mol}^{-1}$ ). The radical  $pK_a$  ( $\text{HOArArO}^\cdot + \text{H}_2\text{O} \rightleftharpoons \text{H}_3\text{O}^+ + ^-\text{OArArO}^\cdot$ ) is measured to be  $7.5 \pm 0.1$ . At pH 12, a reduction potential = 0.448 V vs NHE for the  $^-\text{OArArO}^\cdot/\text{H}^+/\text{HOArArO}^-$  couple is obtained from measurements against the  $\text{Fe}(\text{CN})_6^{3-}/\text{Fe}(\text{CN})_6^{4-}$  reference couple. Subsequently, from the parent  $pK_a$  (9.4, 14.1) and the radical  $pK_a$ , the reduction potential values in the pH range 0–14 are obtained. Some representative values (in V) are: 1.265 (at pH = 0), 0.805 (pH = 7.5), 0.616 (pH = 9.4), and 0.339 (pH > 14). From the reduction potential value at pH = 0, the upper limit of its first O–H bond dissociation energy in the gas phase is estimated to be  $357.7 \text{ kJ mol}^{-1}$ .

### Introduction

During oxidation of a phenolic compound in aqueous or other media, its phenoxyl radical is formed either by the ArO–H bond cleavage (H-atom abstraction) or by one-electron transfer from the phenolate anion to the oxidant. The one-electron reduction potential of the phenoxyl radical from phenol ( $\text{PhO}^\cdot$ ) in aqueous medium (= 0.8 V vs. NHE at pH >  $pK_a$  (= 10),<sup>1–3</sup> or the gas-phase  $\text{PhO}-\text{H}$  bond dissociation energy (BDE =  $368.7 \text{ kJ mol}^{-1}$ )<sup>3</sup> can be taken as benchmark for both reduction potential or BDE for other substituted phenols or phenolic compounds ( $\text{SArOH}$ ). Because all phenolic compounds have at least one parent  $pK_a$  ( $\text{SArOH} + \text{H}_2\text{O} \rightleftharpoons \text{H}_3\text{O}^+ + \text{SArO}^-$ ), at pH below this  $pK_a$  the reduction potential increases with a slope of 0.059 V/pH,<sup>1</sup> and therefore the matrix pH also plays an important role in the oxidation reactions. In general, an electron donating substituent lowers the reduction potential, but the extent of decrease also depends on the substituent position with respect to the C-atom bearing the –OH group. On the other hand, phenols with electron withdrawing substituent have higher reduction potential and thus may resist complete oxidation by milder oxidants. Therefore, the reactivity of any phenol (and its corresponding phenolate anion) or its antioxidant ability under a known oxidative stress can be estimated from a prior knowledge of its  $pK_a$  and the reduction potential of the phenoxyl radical (or equivalently the O–H BDE of the phenol in the gas phase).

Among various types of substituted phenols, compounds with multiple –OH groups on the same or adjacent rings (in fused-ring or polycyclic structures) are considered as potential antioxidants in biological systems.<sup>4,5</sup> Recently, antioxidant and antimutagenic properties have also been reported for resveratrol (3,5,4'-trihydroxy-trans-stilbene).<sup>6</sup> Its multiring (not fused but bridged) polyphenolic structure is quite different from the other class of polycyclic phenolic compounds mentioned above. Thus, its reported antioxidant property probably results from the bridged planar configuration, and this structural feature merits

a detailed investigation. In this case the –HC=CH– bridge is capable of participating in charge delocalization on both the rings; however, similar charge delocalization is also possible even in the absence of the bridge, for example, in a polyphenolic molecule such as 4,4'-biphenol (or 4,4'-dihydroxybiphenyl,  $\text{HOAr}-\text{ArOH}$ ;  $\text{Ar}=\text{C}_6\text{H}_4$ ). The 4,4'-biphenol (4,4'BP) structure has a direct bond between the two halves, and its planar configuration<sup>7</sup> represents the minimum basic molecular geometry for this type of polyphenolic compound. Therefore, 4,4'BP antioxidant ability (i.e., the one-electron reduction potential of its phenoxyl radical) should be a benchmark for other more complex systems such as resveratrol. Additionally, the 4,4'-biphenol structure can also be visualized as a *para*- $\text{C}_6\text{H}_4\text{OH}$  substituted phenol and, therefore, the effect of this substitution on the phenolic (O–H) bond strength may also be taken as indicative of the bond strengths for more complex structures. In the literature; however, no relevant information is yet available either for 4,4'BP or any other bridged polyphenolic compounds regarding their phenolic (O–H) bond strengths, reduction potentials, or the reactivity of the respective phenoxyl radicals, etc. In this study, we have used the pulse radiolysis technique to generate the phenoxyl radical from 4,4'BP in aqueous medium and characterize it by its optical absorption spectra and estimate its  $pK_a$  to find the dependence of its reduction potential against the matrix pH. These results are further extended to estimate the gas-phase dissociation energy of its first O–H bond and related structural characteristics.

### Experimental Section

The 4,4'BP sample (white powder; grade purum,  $\geq 98\%$ ) was obtained from Fluka and was used without further purification. All other chemicals used were AR grade and obtained locally. Nanopure water was used for sample preparation. 4,4'BP has a limited solubility in neutral and acidic pH but is freely soluble in alkaline pH. However, in alkaline pH slow thermal oxidation takes place in the presence of dissolved  $\text{O}_2$ , and appropriate precautions were taken in each set of study. The parent absorption spectra were measured on a Hitachi 330

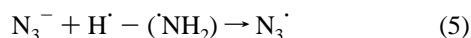
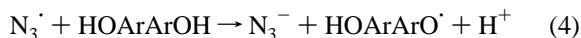
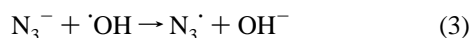
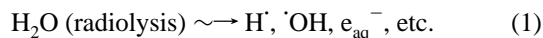
\* Fax: 91-22-5505151. E-mail: tndas@apsara.barc.ernet.in.

spectrophotometer. The 7 MeV electron pulse radiolysis system and the associated kinetic spectrophotometric detection setup used in this study have been described previously.<sup>8</sup> Samples were irradiated in a 1 cm square Suprasil cell. Optical detection of transients was performed within the spectral range of 230–830 nm using a 450 W xenon lamp and a Kratos monochromator blazed at 300 nm coupled to a Hamamatsu R-955 photomultiplier tube. A spectral resolution of  $\approx 3$  nm was routinely achieved, and the effect of scattered light at 250 nm was  $< 2\%$ . Sample replenishment before each pulse was achieved with a flow system, and oscilloscope traces were averaged for both spectral and kinetic measurements. For dosimetry, a  $0.01 \text{ mol L}^{-1}$  ( $\equiv 10 \text{ mol m}^{-3}$ ) aerated  $\text{SCN}^-$  solution was used with the  $G \times \epsilon = 2.59 \times 10^{-4} \text{ m}^2 \text{ J}^{-1}$  at 475 nm.<sup>9</sup> The measured values from pulse radiolysis experiments generally have an uncertainty of  $\pm 10$ – $15\%$ , and it applies to all subsequent results of this study.

## Results and Discussion

**Estimation of Parent  $pK_a$ .** The parent (4,4'BP) absorption spectra were measured between  $\text{pH} = 3$  and  $H_- = 16$ .<sup>10</sup> The solutions were first saturated with  $\text{N}_2$  to prevent any thermal oxidation by  $\text{O}_2$ , especially in the presence of alkali. Generally, for the final pH adjustment phosphate buffer was employed, but at  $\text{pH} \geq 12.5$ , only KOH solution (made  $\text{CO}_3^{2-}$  free with  $\text{Ba}(\text{OH})_2$ ) was used and the solution  $\text{pH}/H_-$  was taken from the prevailing concentration of KOH.<sup>10</sup> From the changes in the absorption characteristics of 4,4'BP, its  $pK_a$  were measured as  $9.4 \pm 0.05$  and  $14.1 \pm 0.10$ . These values are supported by fluorescence results reported in a recent publication from our center.<sup>11</sup> Compared to phenol ( $pK_a = 10$ ), the marginally lower value of the first  $pK_a$  indicates a mild electron withdrawing effect of the *para*- $\text{C}_6\text{H}_4\text{OH}$  substituent in 4,4'BP. However, an increase of  $\sim 5$  pH units for the second  $pK_a$  can result only if its planar conformation<sup>7</sup> is maintained in solution. In the planar geometry, the negative charge that results from the first deprotonation gets completely delocalized over the entire phenolate anion and resists further loss of the second proton, except at very high pH (or  $H_-$ ). For an orthogonal (or nonplanar) conformation of the two rings such a delocalization would be negligible, and even the second  $pK_a$  would be close to the value of 10 (phenolic  $pK_a$ ). In the next section additional supportive evidence for a high value of the second  $pK_a$  or the planar structure is presented.

**Pulse Radiolysis Study.** The azidyl radical ( $\text{N}_3^\cdot$ ) was employed in this study as the one-electron oxidant to generate the phenoxy radical from 4,4'BP.<sup>12–14</sup>  $\text{N}_2\text{O}$  saturated solution containing  $0.015 \text{ mol L}^{-1} \text{N}_3^-$ , few hundred micromolar 4,4'BP,  $5 \text{ mmol L}^{-1}$  phosphate buffer was used in all cases. The appropriate reactions are shown below.



In the presence of  $\text{N}_3^-$ ,  $\text{H}^\cdot$  is also reported to generate the azidyl radical, reaction 5.<sup>15,16</sup> Thus, a direct reaction of  $\text{H}^\cdot$  with 4,4'BP is expected to be negligible and is not considered further. On the other hand,  $G(\text{N}_3^\cdot)$  is then expected to get close to the total

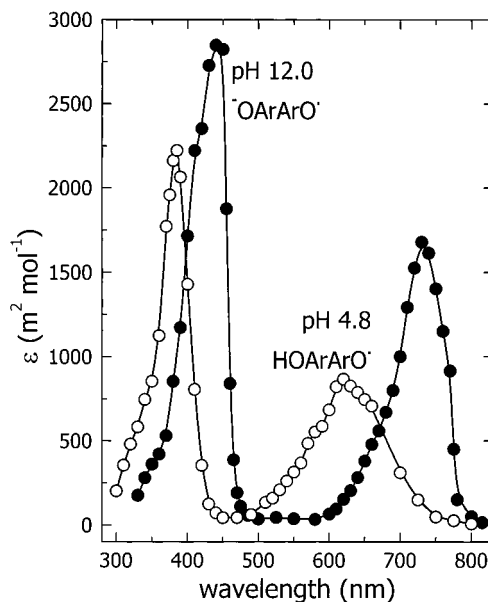


**Figure 1.** Phenoxy radical spectrum at pH 4.8 and 12.0. Absorbed dose 16 Gy in  $\text{N}_2\text{O}$ -saturated solution containing  $0.015 \text{ mol L}^{-1} \text{N}_3^-$ ,  $500 \mu\text{mol L}^{-1}$  4,4'BP,  $0.025 \text{ mol L}^{-1} \text{H}_2\text{PO}_4^-$  buffer (pH 4.8) or  $0.025 \text{ mol L}^{-1} \text{PO}_4^{3-}$  buffer (pH 12.0).

value of  $G(\text{OH}) + G(e_{\text{aq}}^-) + G(\text{H}^\cdot)$  (respectively are 0.28, 0.27 and  $0.06 \mu\text{mol J}^{-1}$ ).<sup>12</sup> For  $0.01 \text{ mol L}^{-1} \text{N}_3^-$  used, an additional  $0.4 \mu\text{mol J}^{-1}$  in  $G(\text{N}_3^\cdot)$  is expected due to enhanced spur scavenging of  $\cdot\text{OH}$  radicals by  $\text{N}_3^-$ , making it  $\sim 6.5 \times 10^{-7} \text{ mol J}^{-1}$ .<sup>17</sup> However, Ye et al.<sup>15</sup> discuss some reduction in the observed yield of  $\text{N}_3^\cdot$  due to its radical–radical reaction in the spur. Therefore, the after-pulse homogeneous  $\text{N}_3^\cdot$  radical concentration available for the 4,4'BP reaction would depend both on the dose used as well as on the prevailing  $\text{N}_3^-$  concentration. For each measurement,  $G(\text{N}_3^\cdot)$  was obtained separately from the prevailing  $\text{N}_3^-$  concentration. The latter was obtained from measured  $\Delta A_{\text{max}}$ , either directly at 274 nm for  $\text{N}_3^\cdot$  radical in  $\text{N}_2\text{O}$  saturated (only)  $\text{N}_3^-$  solution taking  $\epsilon(\text{N}_3^\cdot) = 2025 \text{ L mol}^{-1} \text{cm}^{-1}$ ,<sup>13</sup> or indirectly at 420 nm for  $\text{Fe}(\text{CN})_6^{3-}$  (produced from oxidation of  $\text{Fe}(\text{CN})_6^{4-}$  by  $\text{N}_3^\cdot$  in  $\text{N}_2\text{O}$  saturated  $\text{N}_3^-$  solution containing a few hundred  $\mu\text{mol L}^{-1} \text{Fe}(\text{CN})_6^{4-}$ ) taking  $\epsilon(\text{Fe}(\text{CN})_6^{3-}) = 1070 \text{ L mol}^{-1} \text{cm}^{-1}$ .<sup>18</sup> The  $G(\text{N}_3^\cdot)$  values thus obtained remained close to  $6 \times 10^{-7} \text{ mol J}^{-1}$ .

The absorption spectra of the phenoxy radical were recorded over the pH range 4 to 13. Figure 1 shows the spectra measured at pH 4.8 and 12.0. In both cases two peaks were observed. At pH 4.8, the peaks for the transient radical were observed at 385 nm ( $\epsilon = 2223 \text{ m}^2 \text{ mol}^{-1}$ ) and 620 nm ( $\epsilon = 867 \text{ m}^2 \text{ mol}^{-1}$ ); at pH 12.0, the respective peaks shifted to 445 nm ( $\epsilon = 2850 \text{ m}^2 \text{ mol}^{-1}$ ) and 730 nm ( $\epsilon = 1680 \text{ m}^2 \text{ mol}^{-1}$ ). To check if this spectral change was due to the radical deprotonation, the absorbance at 445 nm was measured against changing matrix pH. Figure 2 shows the plot of  $\Delta A_{445 \text{ nm}}$  vs pH. The variation in  $\Delta A$  could be fitted to a deprotonation step employing the Henderson equation. If the first  $pK_a$  of the phenoxy radical from 4,4'BP (i.e.,  $\text{HOArArO}^\cdot + \text{H}_2\text{O} \rightleftharpoons \text{H}_3\text{O}^+ + \text{OArArO}^\cdot$ ) is assumed to have a value  $\leq 0$ ,<sup>19</sup> then the value  $7.5 \pm 0.1$  from Figure 2 represents the second radical  $pK_a$  for reaction 6.



As discussed later, the absence (at  $\text{pH} < 7.5$ ) or presence (at  $\text{pH} > 7.5$ ) of unit negative charge on the radical species at these pHs was reconfirmed from the change of radical decay kinetics at various ionic concentration. The 6.6 pH unit decrease of the

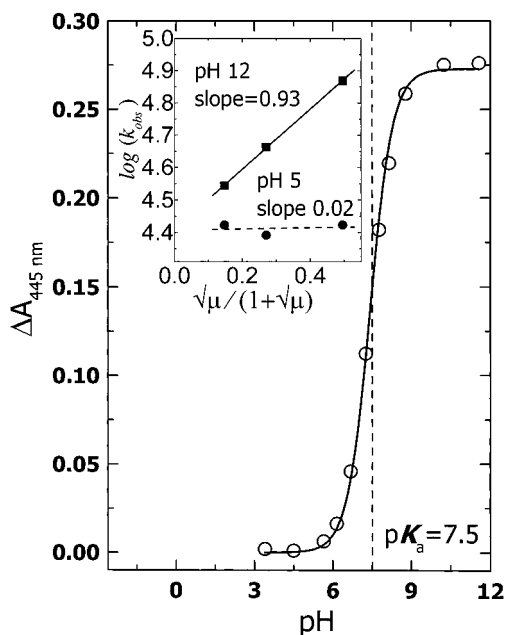


**Figure 2.** Variation of  $A_{445 \text{ nm}}$  (O) against solution pH for conditions as in Figure 1. Solid line represents fitting of Henderson equation for radical deprotonation. Inset: variation of phenoxyl radical decay kinetics  $k_{\text{obs}}$  in a matrix of  $1 \times 10^{-3} \text{ mol L}^{-1} \text{ N}_3^-$ ,  $1 \times 10^{-3} \text{ mol L}^{-1}$  phosphate buffer,  $250 \mu\text{mol L}^{-1}$  4,4'BP,  $\text{N}_2\text{O}$  saturated and with added  $\text{Na}_2\text{SO}_4$  at pH 5 (385 nm) and pH 12 (445 nm).  $\mu = \sum_m c_m z_m^2$  where  $c_m$  is the concentration of ion  $m$  with charge  $z_m$ .

second  $\text{p}K_a$  or increase in its acid strength arises due to the electron withdrawing property of the (*para*)-Ar(4)O $\cdot$  substituent in the radical as compared to the reverse electron donating property of the (*para*)-Ar(4)O $^-$  substituent in the parent. A similar change in the second  $\text{p}K_a$  has been reported for hydroquinone. In this case, the decrease is by almost eight units (from 12 in HOArO $^-$  to 4.0 in HOArO $\cdot$ )<sup>20,21</sup> in the absence of the intervening second -Ar- group.

**Phenoxyl Radical Formation and Decay Kinetics.** The kinetics of phenoxyl radical formation with  $\text{N}_3^-$  as the oxidizing radical was measured at pH 4.8 (385 nm) and pH 12.0 (445 nm). In these experiments, a low dose of 3 Gy was employed and the various solute concentrations in  $\text{N}_2\text{O}$  saturated solutions were as follows:  $0.01 \text{ mol L}^{-1} \text{ N}_3^-$ ;  $15 \text{ mmol L}^{-1}$  phosphate buffer, and  $50\text{--}250 \mu\text{mol L}^{-1}$  4,4'BP. The bimolecular rate constant value of  $3.5 \times 10^9 \text{ L mol}^{-1} \text{ s}^{-1}$  at pH 4.8 increased marginally to  $5.3 \times 10^9 \text{ L mol}^{-1} \text{ s}^{-1}$  at pH 12.0, supporting a faster oxidation of the negatively charged phenolate anion.

In alkaline pH, the kinetics of phenoxyl radical generation by other secondary oxidizing radicals can be employed to measure the charge on the parent molecule. To achieve it, the formation rate constants were measured with  $\text{CO}_3^{2-}$  and  $\text{I}_2^-$  radicals in the presence of increasing amounts of  $\text{Na}_2\text{SO}_4$ . As shown in Figure 3, for each of these radicals at selected pH, the  $\log(k_{\text{obs}})$  was plotted against  $\sqrt{\mu}/(1+\sqrt{\mu})$  where  $\mu$  represents the total ionic strength of the matrix (calculated following the relation  $\mu = 0.5 \times (\sum_i c_i z_i^2)$  where  $c_i$  is the concentration of an ion and  $z_i$  is its charge). Between pH 11 and 13, the slope of the plot following the Debye-Hückel relation (taking  $\alpha = 1$ ) was always found to be close to +1 for these radicals. These results confirm that the charge on the phenolate anion remains -1 (+1 not possible) in this pH range and suggests that the second deprotonation occurs at pH higher than 14. These results reconfirm that the parent molecule maintains the planar conformation in solution. At pH 13, although about 10% dianion

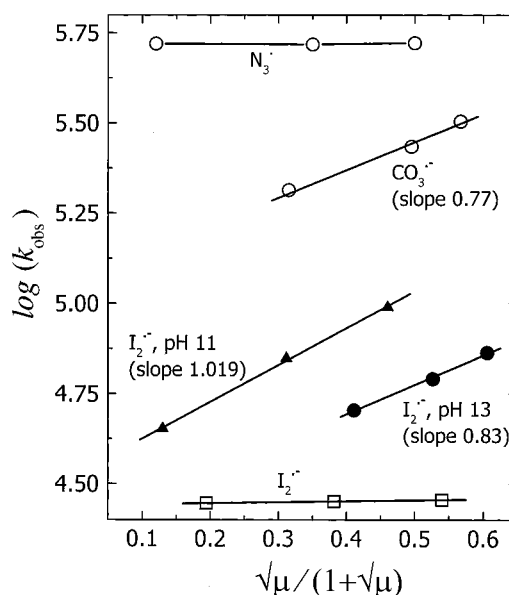


**Figure 3.** Effect of ionic strength due to added  $\text{Na}_2\text{SO}_4$  on the formation kinetics of the phenoxyl radical from 4,4'biphenol. Absorbed dose = 4.5 Gy; pH adjusted with KOH. The  $\text{N}_2\text{O}$  saturated matrix compositions are:  $100 \mu\text{mol L}^{-1}$  biphenol and  $3 \text{ mmol L}^{-1} \text{ N}_3^-$  for the  $\text{N}_3^-$  radical at pH 12;  $200 \mu\text{mol L}^{-1}$  biphenol and  $35 \text{ mmol L}^{-1} \text{ CO}_3^{2-}$  for the  $\text{CO}_3^{2-}$  radical at pH 13;  $100 \mu\text{mol L}^{-1}$  biphenol and  $13 \text{ mmol L}^{-1} \text{ I}^-$  for the  $\text{I}_2^-$  radical at pH 13;  $200 \mu\text{mol L}^{-1}$  biphenol and  $13 \text{ mmol L}^{-1} \text{ I}^-$  for the  $\text{I}_2^-$  radical at pH 11 and  $200 \mu\text{mol L}^{-1}$  biphenol and  $13 \text{ mmol L}^{-1} \text{ I}^-$  for the  $\text{I}_2^-$  radical at pH 8.

contribution is expected in the oxidation process, a slope value close to +1 in both the cases ( $\text{CO}_3^{2-}$  and  $\text{I}_2^-$  radicals) indicates that the respective oxidation rates of the dianion are not significantly higher from that of the monoanion oxidation processes. The slope value remained  $\sim 0$  during oxidation by  $\text{I}_2^-$  at pH below the parent first  $\text{p}K_a$  (and also during oxidation by  $\text{N}_3^-$  radical at pH 13) because one of the reacting species (the parent in the case of  $\text{I}_2^-$  and the radical in the case of  $\text{N}_3^-$ ) was neutral. Thus the Debye-Hückel relation was followed in all cases presented in Figure 3. The individual experimental details are mentioned in the Figure 3 caption.

The phenoxyl radical decay always followed a second-order kinetics, irrespective of the dose, starting solute concentration, pH, or buffer concentration at same ionic strength. The second-order kinetics may arise either due to radical dimerization or radical disproportionation reactions. To quantify the kinetics, the rate was conveniently measured either at 620 nm (pH 4.8) or at 730 nm (pH 12.0), employing a dose of 10 Gy and using  $250 \mu\text{mol L}^{-1}$  4,4'BP,  $1 \text{ mmol L}^{-1} \text{ N}_3^-$ , and  $1 \text{ mmol L}^{-1}$  buffer concentration. A  $2k$  value close to  $4.5 \times 10^8 \text{ L mol}^{-1} \text{ s}^{-1}$  was obtained at pH 5 and  $8.0 \times 10^8 \text{ L mol}^{-1} \text{ s}^{-1}$  at pH 12. The effect of ionic concentration (as added  $\text{Na}_2\text{SO}_4$ ) on radical decay kinetics ( $k_{\text{obs}}$ ) was checked to verify the presence of a negative charge on the radical in alkaline pH. The plot of  $\log(k_{\text{obs}})$  vs  $\sqrt{\mu}/(1+\alpha\sqrt{\mu})$ , where  $\alpha$  is taken as 1.00, in the inset of Figure 2, provides a slope of 0.93 at pH 12.0, but a value close to 0 at pH 4.8. If the measured slope of 0.93 is taken to be approximately 1.0, then, from the Debye-Hückel relation, the negative charge on the phenoxyl radical ( $^-\text{OArArO}^{\cdot}$ ) is confirmed (a +1 charge is not possible in this case). At pH 4.8, the slope value close to 0 confirms the neutral character of the phenoxyl radical (HOArArO $\cdot$ ).

**Reduction Potential of Phenoxyl Radical.** In alkaline pH, if we consider 4,4'BP as a phenol with  $-\text{C}_6\text{H}_4\text{O}^-$  substitution at the para position, then from the overall electron donating

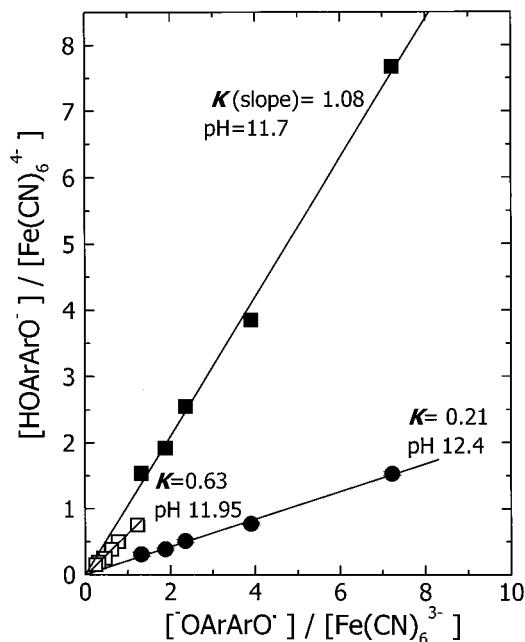


**Figure 4.** Equilibrium oxidation of  $\text{Fe}(\text{CN})_6^{4-}$  by the phenoxyl radical  $^-\text{OArArO}^{\cdot}$  at pH near 12. Measurements made with absorbed dose = 3 Gy,  $\text{N}_2\text{O}$ -saturated matrix containing  $0.02 \text{ mol L}^{-1} \text{N}_3^-$ ,  $0.02 \text{ mol L}^{-1} \text{PO}_4^{3-}$  buffer,  $250 \mu\text{mol} - 2.5 \times 10^{-3} \text{ mol L}^{-1}$  4,4'BP, and  $350 \mu\text{mol} - 2.0 \times 10^{-3} \text{ mol L}^{-1} \text{Fe}(\text{CN})_6^{4-}$ . Variation in matrix pH in the three sets of experiments was made using extra KOH.

nature of this group we expect a lowering of its reduction potential with respect to phenol.<sup>3,5</sup> To judge this extent of reduction,  $\text{N}_2\text{O}$ -saturated solutions at pH 12 containing  $0.05 \text{ mol L}^{-1} \text{N}_3^-$ ,  $0.025 \text{ mol L}^{-1} \text{PO}_4^{3-}$ ,  $200 \mu\text{mol L}^{-1}$  4,4'BP and varying amounts of phenol (between  $2$  and  $15 \times 10^{-3} \text{ mol L}^{-1}$ ) were irradiated employing a 3 Gy dose. The  $^-\text{OArArO}^{\cdot}$  radical yield under these conditions was always close to the projected maximum yield (of  $6 \times 10^{-7} \text{ mol J}^{-1}$ ), indicating that the  $\text{PhO}^{\cdot}$  radical, formed first from oxidation of phenolate anion by  $\text{N}_3^-$ , subsequently oxidized 4,4'BP completely. Absence of any equilibrium electron transfer between the two radicals  $\text{PhO}^{\cdot}$  and  $^-\text{OArArO}^{\cdot}$  suggests that, at pH 12, the reduction potential of the latter is less than 0.6 V. On the other hand, when  $\text{N}_2\text{O}$ -saturated solutions containing  $0.05 \text{ mol L}^{-1} \text{N}_3^-$ ,  $0.025 \text{ mol L}^{-1} \text{KOH}$ ,  $2-5 \times 10^{-3} \text{ mol L}^{-1}$  4,4'BP and  $100-400 \mu\text{mol L}^{-1}$  of TMPD (tetramethyl-*p*-phenylenediamine;  $E^1 = 0.270 \text{ V}$ ) or 4-aminophenol ( $E^1 = 0.22 \text{ V}$ )<sup>5</sup> were irradiated, the  $^-\text{OArArO}^{\cdot}$  radical, formed first in either case, oxidized the latter compounds completely. The respective rate constants,  $9.8 \times 10^8$  and  $1.0 \times 10^9 \text{ L mol}^{-1} \text{ s}^{-1}$ , reflect the close reduction potential values of these compounds. These results also indicated that  $E(^-\text{OArArO}^{\cdot}, \text{H}^+/\text{HOArArO}^-)$  is higher than 0.4 V. Further search for a suitable reference redox couple for equilibrium electron transfer ended with the  $\text{Fe}(\text{CN})_6^{3-}/\text{Fe}(\text{CN})_6^{4-}$  system. Close to pH 12, the equilibrium condition of reaction 7 was achieved using variable concentrations of both 4,4'BP and  $\text{Fe}(\text{CN})_6^{4-}$  (with  $\text{N}_3^-$  as the oxidizing radical). If we assume that in the presence of these solutes (details of concentrations used are indicated in Figure 4 caption) the total yields of the  $^-\text{OArArO}^{\cdot}$  and  $\text{Fe}(\text{CN})_6^{3-}$  radicals remain constant and these radicals react mainly with these solutes, the equilibrium constant  $K$  for reaction 7 is defined by eq 8,<sup>22</sup> and the numerical value of  $K$  is obtained from the slope of the linear plots of the ratio of solute concentrations vs the ratio of radical concentrations. If the value of  $E(\text{Fe}(\text{CN})_6^{3-}/\text{Fe}(\text{CN})_6^{4-})$  at the high experimental ionic strength is taken as  $0.46 \text{ V}$ ,<sup>23</sup> then  $E(^-\text{OArArO}^{\cdot}, \text{H}^+/\text{HOArArO}^-)$

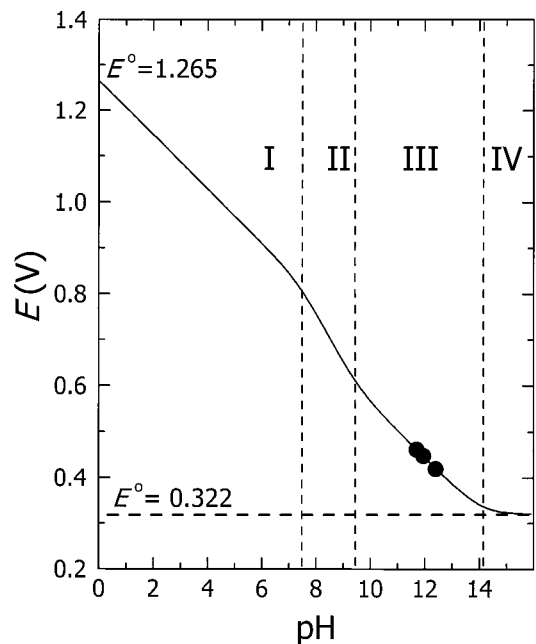
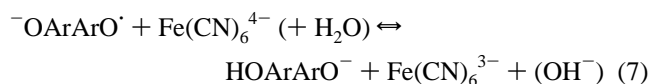


**Figure 5.** Plot of  $E^1$  vs pH for the phenoxyl radical based on eq 10.

is obtained from eq 9.



$$K \approx \frac{[\text{HOArArO}^-] \times [\text{Fe}(\text{CN})_6^{3-}]}{[\text{Fe}(\text{CN})_6^{4-}] \times [^-\text{OArArO}^{\cdot}]}$$

or

$$K \approx \frac{[\text{HOArArO}^-]/[\text{Fe}(\text{CN})_6^{4-}]}{[^-\text{OArArO}^{\cdot}]/[\text{Fe}(\text{CN})_6^{3-}]} \quad (8)$$

$$E(^-\text{OArArO}^{\cdot}, \text{H}^+/\text{HOArArO}^-) =$$

$$E(\text{Fe}(\text{CN})_6^{3-}/\text{Fe}(\text{CN})_6^{4-}) + 0.059 \times \log(K) \quad (9)$$

The reduction potential values obtained at three matrix pH 11.7, 11.95, and 12.4 are 0.463 V ( $K = 1.08$ ), 0.448 V ( $K = 0.63$ ), and 0.422 V ( $K = 0.21$ ), respectively. Using the  $pK_a$  values of the parent 4,4'BP ( $K_{P1} = 4 \times 10^{-10}$  and  $K_{P2} = 7.94 \times 10^{-15}$ ) and the radical ( $K_{1R} \geq 1$  and  $K_{2R} = 3.16 \times 10^{-8}$ ), the reduction potential at any pH ( $= i$ ) is related to the value at pH ( $= 0$ ) by eq 10.

$$E_i = E^0 + 0.059 \times \log(K_{1P} \times K_{2P} + K_{1P} \times [\text{H}^+] + [\text{H}^+]^2) / (K_{1R} \times K_{2R} + K_{1R} \times [\text{H}^+] + [\text{H}^+]^2) \quad (10)$$

Thus, from the three measured  $E^1$  values and using eq 10, a plot of  $E^1$  vs pH is obtained (Figure 5). In this plot the reduction potential increases continuously below pH 14.1. In the four regions marked I to IV, different one-electron reduction couples are best represented as  $\text{HOArArO}^{\cdot}, \text{H}^+/\text{HOArArOH}$  (region I);  $^-\text{OArArO}^{\cdot}, 2\text{H}^+/\text{HOArArOH}$  (region II);  $^-\text{OArArO}^{\cdot}, \text{H}^+/\text{HOArArO}^-$  (region III), and  $^-\text{OArArO}^{\cdot}/^-\text{OArArO}^-$  (region IV). The value increases with a slope  $\approx -0.059 \text{ V pH}^{-1}$  below pH 14 in region III due to a simultaneous single protonation to form the parent molecule; the slope increases further to  $\approx -0.118 \text{ V pH}^{-1}$  in region II as a result of double protonation. However,



the slope in this narrow region actually looks like  $\approx 0.09 \text{ V pH}^{-1}$  because of the effect of nearby (lower) curvatures on both sides. The slope again reverts back to its original value of  $-0.059 \text{ V pH}^{-1}$  at  $\text{pH} \leq 7.5$  (region I) where the radical forms the parent as a result of a single protonation. The actual value of the first  $\text{pK}_a$  of the radical has no effect on this reduction potential vs. pH relation as long as it remains  $\leq 0$ . Some specific reduction potential values are 1.265 V (at  $\text{pH} = 0$ ), 0.805 (pH = 7.5), 0.616 (pH = 9.4), 0.339 (pH = 14.1) and 0.322 (equivalent to pH 15).

**Bond Dissociation Energy of O–H Bond.** The reduction potential of 4-substituted phenols at pH 0 (V vs. *NHE*) has been related to the upper limit BDE ( $\text{kJ mol}^{-1}$ ) of the O–H bond in gas phase by a linear relation (eq 13).<sup>3</sup>

$$\text{BDE} = 236.2 + 96.1 \times E_{\text{pH}=0}^0 \quad (13)$$

This relation was derived from relations in eq 14.

$$\begin{aligned} \Delta H^\circ(\text{SArOH}_g \rightarrow \text{SArO}_g + \text{H}_g) &= \Delta G^\circ(\text{SArOH}_{\text{aq}} \rightarrow \\ &\text{SArO}_{\text{aq}} + 1/2\text{H}_{2(g)} + \Delta G^\circ(1/2\text{H}_{2(g)} \rightarrow \text{H}_g) - \\ &\Delta G^\circ(\text{SArOH}_{\text{aq}} \rightarrow \text{SArOH}_g) + \Delta G^\circ(\text{SArO}_{\text{aq}} \rightarrow \text{SArO}_g) + \\ &T(S^\circ(\text{H}) + \Delta S^\circ(\text{SArO} \rightarrow \text{SArOH})) \quad (14) \end{aligned}$$

In this equation,  $\Delta G^\circ(\text{SArOH}_{\text{aq}} \rightarrow \text{SArO}_{\text{aq}} + 1/2\text{H}_{2(g)})$  is obtained from the  $E^1$  at pH 0;  $\Delta G^\circ(1/2\text{H}_{2(g)} \rightarrow \text{H}_g)$  has a value of 203.0  $\text{kJ mol}^{-1}$ ;  $\Delta G^\circ(\text{SArOH}_{\text{aq}} \rightarrow \text{SArOH}_g) + \Delta G^\circ(\text{SArO}_{\text{aq}} \rightarrow \text{SArO}_g)$  has a value  $\approx 0$ , assuming the solvation of the phenol or the phenoxyl radical is insensitive to the 4-substitution; and the respective values of  $S^\circ(\text{H})$  and  $\Delta S^\circ(\text{SArO} \rightarrow \text{SArOH})$  are 115 and  $-5.98 \text{ J mol}^{-1} \text{ K}^{-1}$ , respectively.

From the reduction potential value of 1.265 V vs *NHE* at pH 0, the upper limit of the first O–H bond dissociation energy for 4,4'BP in gas phase is found to be 357.7  $\text{kJ mol}^{-1}$ . The decrease of  $\sim 11.0 \text{ kJ mol}^{-1}$  in O–H BDE as compared to phenol<sup>3</sup> reflects a significantly enhanced ability of 4,4'BP to scavenge oxidizing radicals under an oxidative stress. More importantly, it also provides the limiting value to which the O–H BDE in bridged polyphenols such as resveratrol can decrease. The reason is as follows. For our comparison, if resveratrol is also taken as a para-substituted phenol (with the  $-\text{CH}=\text{CHC}_6\text{H}_3-3,5-(\text{OH})_2$  group as the substituent) then, first, the intervening  $-\text{CH}=\text{CH}-$  bridge is expected to reduce any terminal substituent electron donating effect<sup>24</sup>, and second, the terminal group with two *meta*-O<sup>-</sup> substitutions may show only mild electron donating property.<sup>24</sup> Near the physiological pH, if protonation occurs, then the resulting *meta*-OH groups may even show a moderate electron withdrawing character.<sup>24</sup>

Continuing with our comparison of the para substituent effect, we find that the reduction potential of the  $^-\text{OAr}^{\text{II}}\text{Ar}^{\text{I}}\text{O}^{\cdot}$  radical is  $\sim 0.3 \text{ V}$  higher than that of the  $^-\text{OAr}^{\text{I}}\text{O}^{\cdot}$  radical produced from 4-hydroxyphenol or hydroquinone.<sup>1</sup> Qualitatively, it indicates that the additional  $-\text{Ar}-$  bridge in 4,4'BP partially offsets the strong electron donating property of the terminal  $^-\text{O}-$  group, and therefore itself has a weak electron withdrawing property. This trend is also observed in our recent measurement of the reduction potential of the  $\text{PhArO}^{\cdot}$  radical from 4-phenylphenol, which was found to be 0.130 V higher than the  $\text{PhO}^{\cdot}$  radical.<sup>2,25</sup> If we consider it also as an example of para substitution on the basic  $-\text{ArO}^{\cdot}$  structure, then the electron withdrawing ability of the terminal  $\text{C}_6\text{H}_5-$  group in the former supports a similar property of the  $-\text{C}_6\text{H}_4-$  group in 4,4'BP above. Following the method proposed by Lind et al.<sup>3</sup> to compare the properties of para substituents in phenols, we calculate a  $\sigma_p^+$  value =  $-0.272$

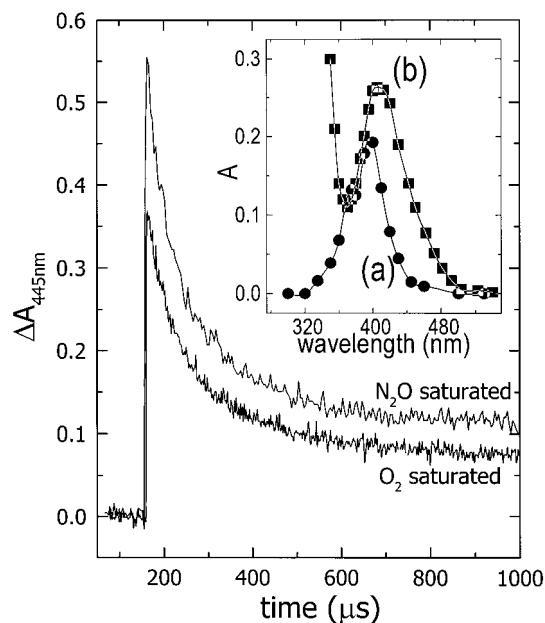


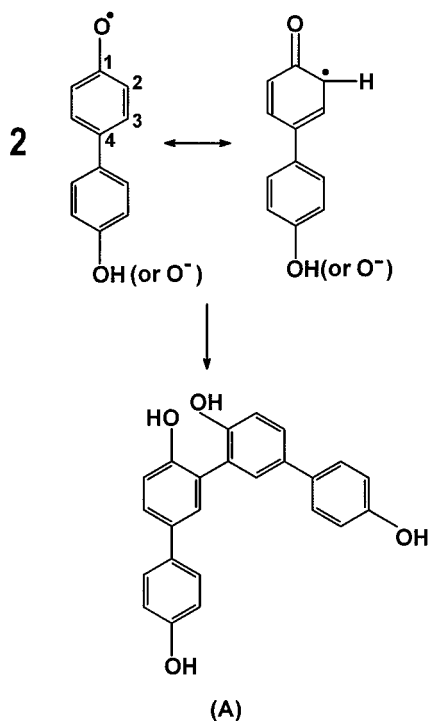
**Figure 6.** Decay of the  $^-\text{OArArO}^{\cdot}$  radical at 445 nm. Measurements made at pH 12, matrix containing  $5 \times 10^{-3} \text{ mol L}^{-1} \text{ N}_3^-$ ,  $5 \times 10^{-3} \text{ mol L}^{-1} \text{ PO}_4^{3-}$  buffer,  $350 \mu\text{mol L}^{-1}$  4,4'BP and absorbed dose = 35 Gy. Inset: Absorption spectra of product obtained from 4,4'BP oxidation. (a) From decay of semioxidized radical, measured after 500  $\mu\text{s}$  at pH 4.8, in  $\text{N}_2\text{O}$  saturated matrix containing  $0.015 \text{ mol L}^{-1} \text{ N}_3^-$ ,  $0.02 \text{ mol L}^{-1} \text{ H}_2\text{PO}_4^-$  buffer,  $200 \mu\text{mol L}^{-1}$  4,4'BP with 14.6 Gy dose. (b) From the thermal oxidation of  $\text{O}_2$  saturated solution at pH  $\sim 14$  containing  $\sim 1 \text{ mol L}^{-1}$  KOH and  $500 \mu\text{mol L}^{-1}$  4,4'BP. Spectrum measured in acidic pH.

for the  $^-\text{OAr}-$  group in 4,4'BP. Once again, it reflects the moderate electron donating property of this group.

**Decay Product of Phenoxyl Radical.** In Figure 6, the decay traces for the phenoxyl radical in the absence and in the presence of  $\text{O}_2$  are compared. As generally observed for other phenoxyl radicals,<sup>26</sup> the decay in this case also was independent of dissolved oxygen concentration. It was also found to be independent of the parent concentration (phenol or phenoxide anion). The second-order decay kinetics therefore arises either from a radical dimerization reaction or from a disproportionation of two radicals leading to the regeneration of the parent 4,4'BP and formation of the oxidized quinone species. In the case of dimerization, as shown in Scheme 1, the reaction can take place at the C2 atom (with respect to the phenolic group) starting from the cyclohexadienone species and the subsequent 1–3 shift of the respective H-atoms to the O-atoms in each half can generate the “all phenolic” structure **A** (2,2'-dihydroxy-5,5'-di-(4-hydroxyphenyl)-biphenyl). It may be noted that, other centers where the dimerization can take place are the C4 atom on the same ring (but will be denied a subsequent H-atom shift) or at the conjugated C atoms on the other ring; dimerization may proceed either symmetrically or otherwise. However, the symmetric 2–2' dimerization in Scheme 1 is proposed as the most probable mode of phenoxyl radical decay based on the following observations.

The absorption spectrum of the product of phenoxyl radical decay is shown in the inset of Figure 6 (curve a). In the case of thermal oxidation of an alkaline solution of 4,4'BP in the presence of dissolved  $\text{O}_2$ , the product spectrum shown in Figure 6 inset (curve b) has a slightly different absorption profile with its broad peak centered around 408 nm. The latter process is expected to produce the quinone-type structure ( $\text{OArArO}$ ). However, only this product reacts with  $\text{S}_2\text{O}_4^{2-}$  to regenerate the parent 4,4'BP phenolate anion just as quinone ( $\text{OArO}$ ) gets

## SCHEME 1: Possible Decay Reaction of the Phenoxy Radical from 4,4'BP



reduced to hydroquinone (HOArOH). Therefore, a comparison of the two spectra in the inset of Figure 6 indicates that the radical dimerization reactions may dominate the decay of phenoxy radical from 4,4'BP and then  $G(\text{Dimer}) \approx 0.5 \times G_{\text{phenoxy radical}}$ . An intense absorption such as this ( $\epsilon_{395 \text{ nm}} = 4450 \text{ m}^2 \text{ mol}^{-1}$ ) is expected for an extended planar four-ring conjugated structure similar to A in Scheme 1. Dimerization at other C atoms would lead to varying degrees of structural strain in the resulting dimers. It may be noted that confirmation of the degree of different types of dimerization and the nature of each product are possible only after their separation by HPLC and comparison with synthesized standard sample(s) in each case. In the absence of necessary support from appropriate facilities, the end product(s) could not be identified. However, the objectives and results of this study are not affected or influenced by the absence of these details.

**Acknowledgment.** I thank my colleagues Dr. Devidas Naik for the biphenol sample, Dr. Haridas Pal for his fluorescence

results, Mr. Vijendra Rao for technical help at the LINAC facility, and Dr. Tulsi Mukherji for a review of the manuscript. I also thank the referees for various suggestions and comments.

## References and Notes

- (1) Wardman, P. *J. Phys. Chem. Ref. Data* **1989**, *18*, 1637.
- (2) Das, T. N.; Huie, R. E.; Neta, P. *J. Phys. Chem. A* **1999**, *103*, 3581.
- (3) Lind, J.; Shen, X.; Erikson, T. E.; Merényi, G. *J. Am. Chem. Soc.* **1990**, *112*, 479.
- (4) Jovanovic, S. V.; Hara, Y.; Steenken, S.; Simic, M. G. *J. Am. Chem. Soc.* **1995**, *117*, 9881.
- (5) Steenken, S.; Neta, P. *J. Phys. Chem.* **1982**, *86*, 3661.
- (6) Jang, M.; Cai, L.; Udeani, G. O.; Slowing, K. V.; Thomas, C. F.; Beecher, C. W. W.; Fong, H. H. S.; Farnsworth, N. R.; Kinghorn, A. D.; Mehta, R. G.; Moon, R. C.; Pezzuto, J. M. *Science* **1997**, *275*, 218.
- (7) (a) Wheland, G. W. *Advanced Organic Chemistry*; John Wiley and Sons: New York, 1957; pp 202–207. (b) Gould, E. S. *Mechanism and Structure in Organic Chemistry*; Holt: New York, 1959; pp 20–21 and 50–53. (c) March, J. *Advanced Organic Chemistry*, 4th ed.; John Wiley and Sons: New York, 1992; pp 101–102.
- (8) Guha, S. N.; Moorthy, P. N.; Kishore, K.; Naik, D. B.; Rao, K. N. *Proc. Indian Acad. Sci. (Chem. Sci.)* **1987**, *99*, 261.
- (9) Buxton, G. V.; Stuart, C. R. *J. Chem. Soc., Faraday Trans.* **1995**, *91*, 279.
- (10) Yagil, G. *J. Phys. Chem.* **1967**, *71*, 1034.
- (11) Mohanty, J.; Pal, H.; Sapre, A. V. *Bull. Chem. Soc. Jpn.* **1999**, *72*, 2193.
- (12) Buxton, G. V.; Greenstock, C. L.; Helman, W. P.; Ross, A. B. *J. Phys. Chem. Ref. Data* **1988**, *17*, 513.
- (13) Alfassi, Z. B.; Prutz, W. A.; Schuler, R. H. *J. Phys. Chem.* **1985**, *89*, 3359 and *J. Phys. Chem.* **1986**, *90*, 1198.
- (14) Neta, P.; Huie, R. E.; Ross, A. B. *J. Phys. Chem. Ref. Data* **1988**, *17*, 1027.
- (15) Ye, M.; Madden, K. P.; Fessenden, R. W.; Schuler, R. H. *J. Phys. Chem.* **1986**, *90*, 5397.
- (16) Deeble, D. T.; Parsons, B. J.; Johnson, G. R. A. *Radiat. Phys. Chem.* **1990**, *36*, 487.
- (17) Schuler, R. H.; Hartzel, A. L.; Behar, B. *J. Phys. Chem.* **1981**, *85*, 192.
- (18) Das, T. N.; Dhanasekaran, T.; Alfassi, Z. B.; Neta, P. *J. Phys. Chem. A* **1998**, *102*, 280.
- (19) Dixon, W. T.; Murphy, D. *J. Chem. Soc., Faraday Trans. 2* **1976**, *72*, 1221.
- (20) Dean, J. A. *Lange's Handbook of Chemistry*, 14th ed.; McGraw-Hill: New York, 1992; Table 8.8.
- (21) Adams, G. E.; Michael, B. D. *Trans. Faraday Soc.* **1967**, *63*, 1171.
- (22) (a) Meisel, D.; Neta, P. *J. Am. Chem. Soc.* **1975**, *97*, 5198. (b) Patel, K. B.; Willson, R. L. *J. Chem. Soc., Faraday Trans. 1* **1973**, *69*, 814. (c) Meisel, D.; Czapski, G. *J. Phys. Chem.* **1975**, *79*, 1503.
- (23) Hanania, G. I. H.; Irvine, D. H.; Eaton, W. A.; George, P. *J. Phys. Chem.* **1967**, *71*, 2022.
- (24) March, J. *Advanced Organic Chemistry*, 4th ed.; John Wiley and Sons: New York, 1992; pp 278–280.
- (25) Das, T. N.; Neta, P. *J. Phys. Chem. A* **1998**, *102*, 7081.
- (26) Jin, F.; Leitich, J.; von Sonntag, C. *J. Chem. Soc., Perkin Trans. 2* **1993**, 1583.